Focused Gaussian Beams for Seismic Imaging

Robert L. Nowack; Dept. of Earth and Atmos. Sci., Purdue University*

Summary

The application of focused Gaussian beams is investigated for the seismic imaging of common-shot reflection data. The focusing of Gaussian beams away from the source and receiver aperture adds flexibility to beam imaging algorithms allowing for the narrowest portions of the beams to occur at the depth of a specific target structure. This minimizes the number of beams required to form an image at the target depth. The beam fronts at the beam-waists are also planar leading to more stable beam summations for imaging. To match with the surface data, a quadratic phase correction is required for the local slant-stacks of the data. Imaging using focused Gaussian beams is tested using a single shot gather for a model with 5 scatterers at different depths. The approach is then tested for a single shot gather from the Sigsbee2A model. In all cases, the beams can be focused to a particular target depth, but proper imaging still results for other depths as well.

Introduction

Summations of Gaussian beams over either initial take-off angle or position along an initial surface have been applied for the computation of high frequency seismic wavefields in smoothly varying inhomogeneous media (see for example, Popov, 1982; Cerveny et al. 1982; Nowack and Aki, 1984). Reviews of Gaussian beam summation have been given by Cerveny (1985a,b), Babich and Popov (1989), and more recently by Popov (2002), Nowack (2003), Cerveny et al. (2007) and Bleistein (2007). An advantage of summations using Gaussian beams to construct more general wavefields is that the individual Gaussian beams have no singularities along their paths, no two-point ray tracing is required and triplicated arrivals are naturally incorporated into either forward or inverse modeling. More recently over-complete frame-based Gaussian beam summations have been developed based on window and wavelet transforms to address some of the issues related to completeness of beam summations (Lugara et al., 2003). In an over-complete frame based approach, the wavefield is decomposed into beam fields that are localized both in position and direction. Although an orthonormal basis cannot be formed using a Gabor frame, an over-complete frame expansion can be constructed which has the added benefit of providing redundancy in the expansion (Feichtinger and Strohmer, 1998; Hill; 1990, 2001; Hale, 1992). Here curved initial beams are used to decompose the seismic data and these are then propagated into the subsurface using focused Gaussian beams. The advantage of using focused beams for a target structure at a specific depth is that fewer beams are required for that image depth.

Recent true amplitude migration formulations using Gaussian beams have used with beams traced from the scattering points up to the surface with the beam-waists specified at the scattering points (Protasov and Cheverda, 2005; 2006). However, it is more economical to launch beams from the source and receiver positions down into the subsurface since there are fewer source and receiver locations than subsurface scattering points, and this minimizes the amount of beam tracing required. In order to locate the beam-waists in the subsurface when the beams are launched from the source and receiver aperture, then generally curved beam fronts are required along the source and receiver aperture. A detailed description of the focused Gaussian beam algorithm is provided by Nowack (2008).

Examples

In order to test the focusing beam migration formulation, two examples are given. The first application has 5 compact sources located at depths of 8,000, 12,000, 16,000, 20,000 and 24,0000 ft at a distance of 40,000 ft from the left side of the model. The background velocity model has two layers. The first layer has a thickness of 6000 ft with a

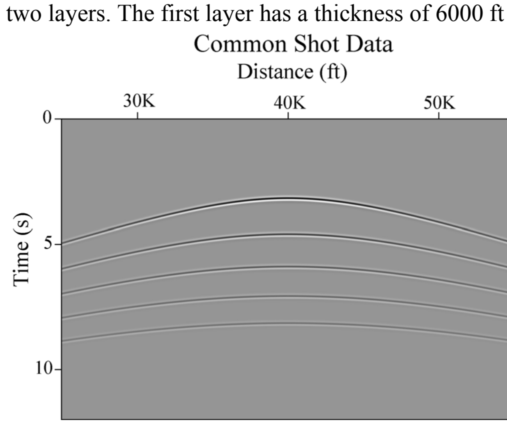

Figure 1. Computed common-shot data is shown for a shot point on the surface at a position of 40,000 ft. The receiver array is from 25,000 ft to 55,000 ft. Diffractions from 5 compact scatterers are shown each with a horizontal position of 40,000 ft and depths of 8,000, 12,000, 16,000, 20,000 and 24,000 ft.

constant velocity of 5000 ft/sec. The second layer goes from 6000 ft to 30,000 ft in depth with a vertical velocity gradient of .15. The shot position is located along the surface at a horizontal position of 40,000 ft from the left side of the model. The receiver array is from 25,000 ft to 55,000 ft on the surface. Figure 1 shows the computed wavefield from the 5 compact scatterers. The sampling rate is .008 sec and the peak frequency of the data is 5 Hz.

Figure 2A shows the partial image of the data from a single vertically propagated Gaussian beam with the planar wavefront at the surface. For simplicity the source side Green's function is constructed separately using Gaussian beams that are planar at the source location for all the examples given. Note on the figure that the images of the diffractors are curved and increase in width with depth. Figure 2B shows the partial image of the common shot data in Figure 1 using a single vertical Gaussian beam at a

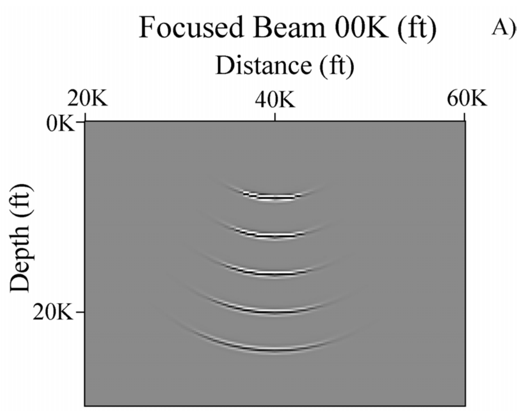

Figure 2A The partial image of the common shot data in Figure 1 using a single vertical Gaussian beam at a receiver position at 40,000 ft using a beam with a planar beam-waist at the surface.

receiver position at 40,000 ft using a focused beam with the beam-waist at a depth of 12,000 ft. Now the diffractor at a depth of 12,000 ft is the most focused using a single beam with the images of the other diffractors being broader and generally curved. Figure 2C shows the partial image of the common shot data in Figure 1 using a single vertical Gaussian beam at a receiver position at 40,000 ft using a focused beam with the beam-waist at a depth of 16,000 ft. Now the diffractor at a depth of 16,000 ft is the most focused using a single beam with the images of the other diffractors being broader and curved.

Figure 3A shows the partial image of the common shot data in Figure 1 using receiver beams centered on 40,000 ft now launched at all angles, each with the beam-waist shifted approximately 16,000 ft. This results in spherical images of all 5 scatterers and indicates that the imaging is being properly applied even with curved and broadened beams at the other depths. Using focusing beams with other beam-waist locations gives similar imaging results.

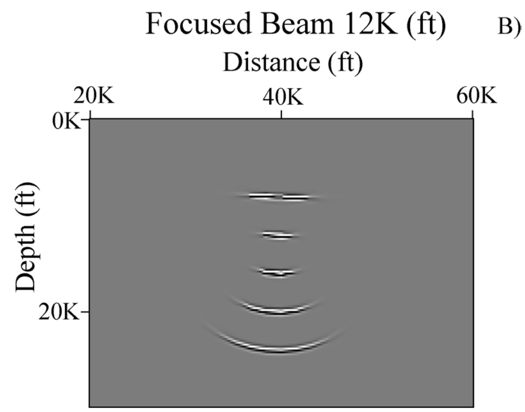

Figure 2B The partial image of the common shot data in Figure 1 using a single vertical Gaussian beam at a receiver position at 40,000 ft using a focused beam with a beam-waist at a depth of about 12,000 ft.

Figure 3B shows the complete Gaussian beam image for the single shot gather from Figure 1 using beams from all beam center locations launched at all angles, each with the beam-waist shifted approximately 16,000 ft. This results in focused images of all 5 scatterers and indicates that the imaging is being properly applied even with the shifted beam-waists of the individual beam components. Using focusing beams with other beam-waist locations gives similar imaging results.

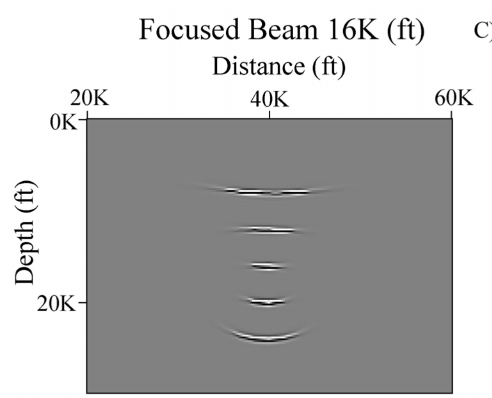

Figure 2C The partial image of the common shot data in Figure 1 using a single vertical Gaussian beam at a receiver position at 40,000 ft using a focused beam with a beam-waist at a depth of about 16,000 ft.

The focusing beam migration approach is now applied to a single shot gather from the Sigsbee2A data set. In order to test the focused beam approach, a single shot gather with a shot location at 6,325 ft from the left edge of the model is used. The receiver array starts at the shot location and has a maximum offset of 26,025 ft with a spacing of 75 ft. The background velocity model has the first layer from the surface down to the seafloor with a velocity of 5000 ft/sec. The second layer goes from seafloor to 30,000 ft in depth with a linear gradient of .3. A salt dome exists in the middle and right parts of the model, but for the initial tests here only a shot gather away from the salt dome is used.

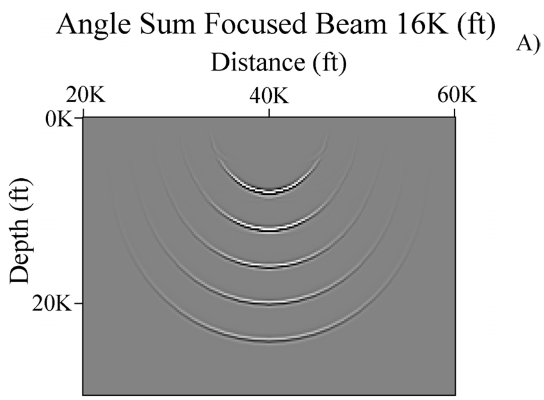

Figure 3A The partial image of the common shot data in Figure 1 using receiver beams centered on 40,000 ft now launched at all angles, each with the beam-waist shifted approximately 16,000 ft. This results in spherical images of all 5 scatterers and indicates that the imaging is being properly applied even with the shifted beam-waists of the individual beam components.

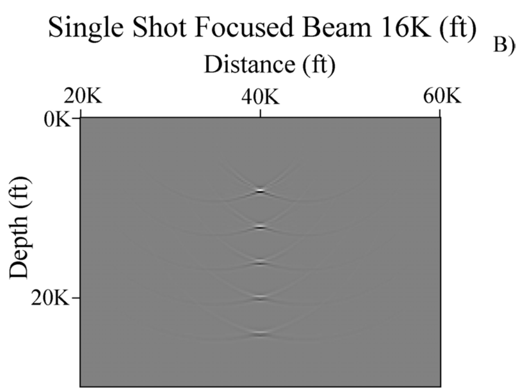

Figure 3B The Gaussian beam image using the complete single shot gather is shown in Figure 1 with beams from all beam positions launched at all angles, each with the beam-waist shifted to approximately 16,000 ft. This results in focused images of all 5 scatterers and indicates that the imaging is being properly applied even with the shifted beam-waists of the individual beam components.

In Figure 4A, the partial imaging for a single Gaussian beam is shown with the planar beam-waist at the receiver depth. As in the earlier examples the source side Green's function is constructed separately using Gaussian beams that are planar at the source location. The receiver Gaussian beam has an initial location near the source and

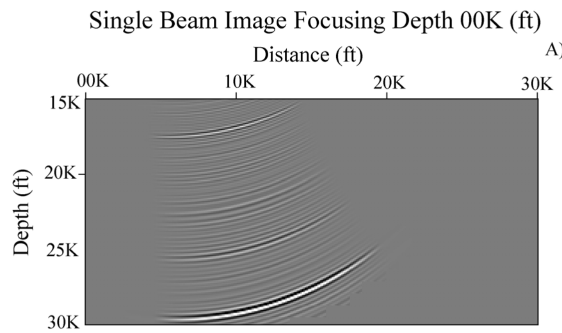

Figure 4A This shows the partial imaging result for a single Gaussian beam with the beam-waist at the surface along the receiver array for a single shot gather from the Sigsbee2A dataset.

the partial image for a beam with a slight angle from the vertical is shown. As in the earlier example, when the beam-waist is at the receiver depth, then curved beam fronts result which broaden with depth over the depth range of the model shown between 15,000 and 30,000 ft. This is typical of standard implementations of Gaussian beam migration. However, in regions of a complicated

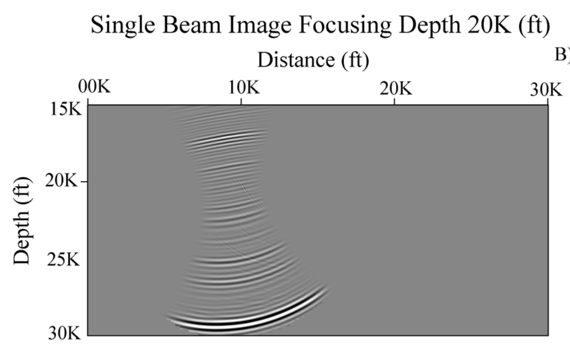

Figure 4B This shows the partial imaging result for a single Gaussian beam with the beam-waist shifted to about 20,000 ft in depth for a single shot gather from the Sigsbee2A dataset.

background medium, the medium itself can cause additional focusing of the beams.

Figure 4B shows the partial imaging results for a single Gaussian beam with the beam-waist shifted to about 20,000 ft in depth. At this depth the narrowest part of the beam image occurs and also with a planar beam front. If the target structure were located at this depth, then fewer beams would be required to form a complete image. Also the beam images would have planar beam fronts at this depth leading to more stable images. However, as shown in Figure 4B, at other depths the partial beam image results in curved and broader beam fronts.

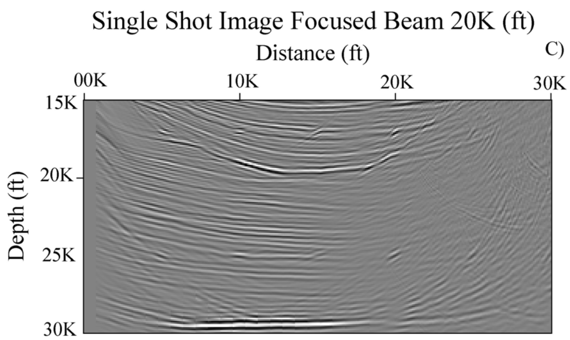

Figure 4C The Gaussian beam image using a complete single shot gather from the Sigsbee2A dataset with the shot location at 6325 ft using beams from all receiver positions launched at all angles each with the beam-waist shifted approximately 20,000 ft.

Figure 4C shows the complete imaging result for a single shot gather when focused Gaussian beams are used with the beam-waists shifted approximately 20,000 ft from the receiver aperture. The shot location is at 6325 ft from the left edge of the model. Although only one of the 500 shots available in the Sigsbee2A dataset is used, the single shot image using focused Gaussian beams shows a number of the subsurface features for this part of the Sigsbee2A reflectivity model. Even though the beam-waists are specified for a depth of about 20,000 ft, the focused beam formulation still properly accounts for the variable curvature and beam widths at all depths of the image. When using other focusing depths, or with beam-waists at the surface, the simple shot images are all very similar to that shown in Figure 4C. The advantage of using the focused beams is that for a target structure at a specific depth, fewer beams will be required to form a stable image. The results shown here are again for a smooth part of the Sigsbee2A background model well away from the salt dome structure. In a more complicated part of the model, focused beams could be designed to compensate for the focusing effects of the background model, in addition to minimizing the number of beams required for imaging. However, this needs to be further explored in future work.

Conclusions

The application of focused Gaussian beams has been investigated for seismic imaging. The shifting of the beam-waists away from the source and receiver aperture adds flexibility to Gaussian beam algorithms allowing for the narrowest portions of the beams to occur at the depth of a specific target structure. This minimizes the number of beams required to form an image at this target depth. Also, at the beam-waists the beam fronts are planar leading to more stable beam summations for imaging. To match with the surface data, a quadratic phase correction is required for the local slant-stacks of the data. Using the same local slant stacks of the data for the different imaging depths, only a single focusing depth can be specified. Imaging using focused Gaussian beams was tested using a single shot gather for a model with 5 scatterers at different depths. The approach was then tested for a single shot gather from the Sigsbee2A model. In all cases, the beams can be focused to a particular target depth, but proper imaging still results for other depths as well.

Acknowledgments

This work was supported in part by the National Science Foundation and partly by the sponsors of the Geo-Mathematical Imaging Group (GMIG) at Purdue University.